ISSN 1392–1320 MATERIALS SCIENCE (MEDŽIAGOTYRA). Vol. 20, No. 1. 2014

Device for Controlled Distribution of FePt Nanoparticles Formations in a Stream of Liquid Medium under Influence of Magnetic Field

Karolis ŠILEIKA [1], Yoshitaka KITAMOTO [2], Bronius BAKŠYS [1], Inga SKIEDRAITĖ [1] *

[1] *Department of Mechatronics, Faculty of Mechanical Engineering and Mechatronics, Kaunas University of Technology, Kęstučio 27, LT-44312 Kaunas, Lithuania*
[2] *Tokyo Institute of Technology, 4259 Nagatsuta-cho, Midori-ku, Yokohama, Kanagawa, 226-8503, Japan*

crossref http://dx.doi.org/10.5755/j01.ms.20.1.3371

Received 30 July 2011; accepted 12 May 2013

In this research paper a design of magnetic device comprising Halbach arrays which maximizes the magnetic forces acting on magnetic nanoparticles and which can be used for successful steering of said particles to a zone of interest and captured thereat while exhibiting a certain flow and accumulation pattern after injection into a stream of a liquid medium is presented. The aim was to investigate efficiency of such design of a magnetic device for application in magnetic targeting techniques. The presented construction was assembled from 10 magnetic elements having the same dimensions and residual magnetic field, and casing of Plexiglas material. Aggregating of clusters of FePt nanoparticles was evidently successful at preferable region located between two opposing parts of a magnetic device, which was tested for flow rates of (1 – 10) mL/min of main stream medium. To simulate the viscosity of blood a 1.5 % PVP 90 solution was used as the flowing medium. The shallow depth of targeting was chosen for practical reason: to ensure a maximum visibility of particle "steering" pattern obtainable by the magnetic device consisting of two adjacent parts comprising Halbach arrays.

Keywords: FePt nanoparticles, Halbach array, magnetic drug targeting, magnetic particles flow.

1. INTRODUCTION

Drug targeting referring here to an active drug targeting is a therapeutic technique, which requires guidance of drug carriers to specific site in a manner such that its major fraction interacts exclusively with the target tissue at the cellular or subcellular level. Typically the intended drug and a suitable magnetically active component are formulated into a pharmacologically stable compound. This compound is injected through an appropriate blood vessel supplying the targeted zone in the presence of an external magnetic field with sufficient field strength and gradient to retain the carrier at the target site. The focused administration of drugs is carried out by use of magnets to direct drug carriers of appropriate size and magnetic properties to specific sites in human body to treat tumours, infections, blood clots, for local hyperthermia and other [1 – 10]. Such administration can reduce unwanted distribution of drugs thus minimizing side effects such as caused by systematically administered chemotherapy [6].

The distance from the magnets to the locations where particles are still effectively captured in particular depends on the vascularization of target region [7], the applied magnetic field and magnetic field gradient. Later two decrease rapidly with increase of distance from magnets; therefore insufficient reach becomes one of the major limits of the applicability of magnetic drug delivery [4, 8, 11 – 13]. In other words, technically, it is difficult to build up sufficient field strength that focuses on a small area and is able to counteract the linear blood-flow rates in the tissue (10 cm/s in arteries and 0.05 cm/s in capillaries [1]).

Basic shape permanent magnets or electromagnets are commonly used to pull particles into the target tissue by placing magnets in close proximity to the target zone so the magnetic drug carriers could be accumulated at a predetermined site. Strength of used magnets and magnetic field gradient varies from 70 mT to 2.2 T and from 0.03 T/m to 100 T/m, respectively [8 – 10, 14]. To date in human clinical trials [1] using 100nm diameter particles a focusing depth of 0.5 cm has been achieved. In animal experiments reported targeting depth was up to 12 cm [15] using 0.2 T – 0.8 T strength magnets and 500 nm – 5 μm magnetic particles. Restricted treatment depths and thus focusing accuracy of drug carriers mean that only a fraction of patients could be treated with magnetic drug delivery.

Most active magnetic drug targeting systems are based on pull forces generated by a single permanent magnet placed near the target tissue. The use of superconducting magnets capable of producing high magnetic fields has been suggested as a way to reach deep locations in the body. Nevertheless, under conditions of a magnetically non-saturated particle the magnetic force on the particle is proportional to both the external magnetic field and the magnetic field gradient. With increasing external magnetic field the particle eventually will reach magnetic saturation thereafter the magnetic force will be proportional only to the magnetic field gradient [4]. With the more powerful magnets, the magnetic field tends to be homogeneous over the target site, resulting in a small field gradient. Hence, increasing the magnetic field by applying a stronger magnet will not necessarily increase the magnetic force on a magnetic particle.

Magnetic implants [4, 16, 17] within a target zone in blood vessels were employed as an alternate way to increase magnetic drug targeting strength in deep tissues. The implanted materials served to locally increase the

* Corresponding author. Tel.: +370-37-300902; fax.: +370-37-323461.
E-mail address: *inga.skiedraite@ktu.lt* (I. Skiedraitė)

magnetic field gradients when an external magnetic field is applied. Nevertheless, this method also lacks solid research data on its effectiveness.

As main issue here is sufficiently large magnetic field gradient at a certain distance from its source the magnetic force on a single ferro-magnetic particle is considered as [9]

$$\overrightarrow{F_M} = \frac{4\pi a^3}{3} \times \frac{\mu_0 \chi}{1 + \chi/3} \left(\frac{\partial \vec{H}}{\partial \vec{x}} \right) \vec{H} = \frac{2\pi a^3}{3} \times \frac{\mu_0 \chi}{1 + \chi/3} \nabla \left\| \vec{H} \right\|, \quad (1)$$

where $\vec{H}$ is the strength of magnetic field [A/m], χ is the magnetic susceptibility, and $\mu_0 = 4\pi \times 10^{-7}$ is the permeability of vacuum, a is the radius of the particle [m], ∇ is the gradient operator [1/m], and $\partial \vec{H} / \partial \vec{x} \neq 0$ is the Jacobian matrix of $\vec{H}$ and both are evaluated at the location of the particle. The first relation shows that a partially varying magnetic field ($\partial \vec{H} / \partial \vec{x} \neq 0$) is required to create magnetic forces. It also shows that the force on a single particle is directly proportional to its volume. The second relation, which is equivalent to the first one, states that the force on particles is along the gradient of the magnetic field intensity squared – i. e. ferro-magnetic particle will always experience a force from low to high applied magnetic field.

If considering a Halbach array composed of permanent rectangular sub-magnets arranged in a cross formation each being magnetized uniformly in a given direction then two independent variables are considered: a number of magnets per wavelength R and total number of wavelengths W in an array [18]. As number of wavelengths increases, the magnetic field of each array becomes stronger but the magnetic field lines exhibit smaller extrusions outside the magnetic array before returning. Thus the force becomes stronger but over a smaller distance. If the strength of a Halbach array is unrestricted, then the magnetic force can be increased simply by using stronger magnets. However there are practical constraints on the available strengths of permanent magnets as well as regulatory safety constraints on the strength of the magnetic field that can be applied across the human body.

The magnetic field from two or more magnets can be added together to establish the net magnetic field, which is a standard assumption in the design of Halbach arrays [12, 18 – 20]. It is true as long as the magnetic field arising from the combination of sub-magnets does not cause partial or complete demagnetization or magnetization reversals [21]. The design presented in this paper does not generate demagnetizing fields strong enough to cause partial or complete demagnetization of the sub-magnets.

So far Halbach arrays have been implemented only for near surface magnetic focusing [12, 14] but not for deep reach. The research presented here aims to investigate the magnetic drug delivery device, which design is based on Halbach arrays [12, 18 – 20], in particular to investigate the performance of mentioned device.

2. MATERIALS AND METHOD

A problem of optimal magnetic assembly design with a predetermined number of elements is considered here in this research. Construction of a strong Halbach arrays with 10 elements is feasible, as it is shown in the experiment. Since generating sufficient force at depth remains a challenge [8, 11, 13] as a specific goal was chosen firstly to investigate trajectory of FePt particle and aggregate stability at a shallow depth in between two opposing parts, designed as Halbach arrays, of the magnetic device.

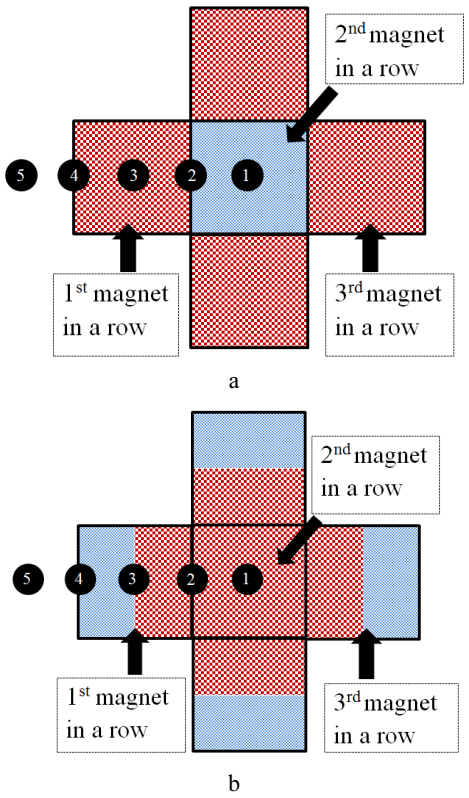

Fig. 1. Configuration of poles (red large checkers – S, blue fine checkers – N) and measurement points 1 – 5 (where each measurement point is separated by 10 mm, and 1st measurement point is in the center of each assembly) in between a) the top block and b) the lower block

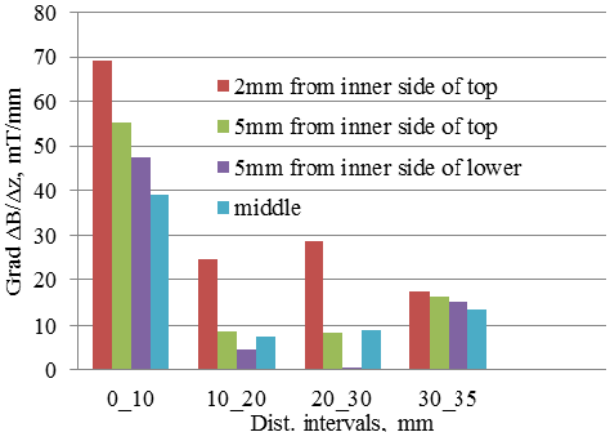

Fig. 2. The magnetic field induction gradient plot

The top part magnets (Fig. 1, a) and lower part magnets (Fig. 1, b) are presented as facing the inner side of the assembly of the experimental device. Such arrangement gives a strong magnetic field near its surface, specifically near the middle magnet of the top part because the magnetic lines have a definite and convenient path to follow. Each

block consists of 5 NdFeB magnets (20 × 20 × 20) mm^3 each having remnant magnetization of around 0.6 T. The design is such that unless both parts are used simultaneously effectiveness of aggregation of FePt particles at a predetermined site is considerably lower.

As it can be seen from Fig. 2 such arrangement gives significantly stronger magnetic field gradient at the 0 mm – 10 mm interval section, where at the relative distances of measurements line between the two blocks varies. By plotting magnetic field gradient values (Fig. 2) one can predict that most efficient capturing of particles will be achieved at the distance interval from point 1 to point 2 (distance interval: 0 mm – 10 mm).

When these two assemblies were positioned to face one another at the distance of more than 20 mm, the two parts of the device exhibited a strong repulsion, but at the distance of less than 20 mm repulsion was replaced by a strong attraction.

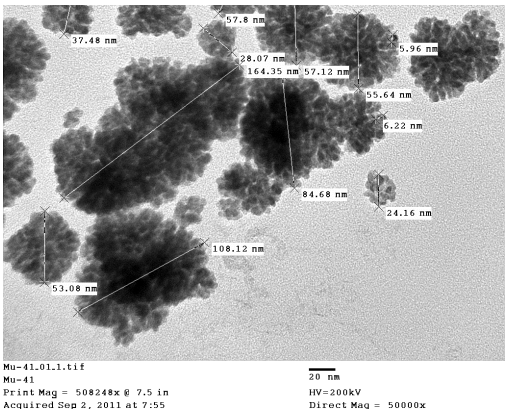

a

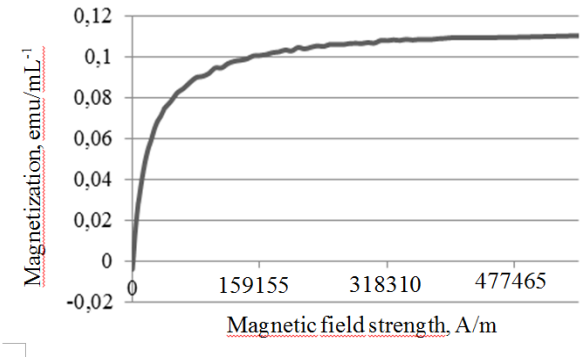

b

Fig. 3. Particles, comprising the used magnetic fluid: a – clusters of FePt particles from used sample; b – magnetization curve of sample's particles

Because the aim was to investigate the operation of the magnetic device, in this case magnetic particles (custom tailored in Tokyo Institute of Technology, prof. Y. Kitamoto's laboratory) comprising the injectable magnetic suspension did not have any coating as it was not necessary. Although it is known that chemical stability of magnetic nanoparticles is possible to achieve by appropriate coating of for example biocompatible dextran matrix [22] so it would be safe to use in human vascular system. FePt particles (Fig. 3, a, b) where mixed with distilled water to form an injectable magnetic solution. The solution was dominant by clusters of FePt particles instead of singular not agglomerated particles.

The experimental setup consisted of supply of 1.5 % PVP solution (as the flowing liquid medium), a roller pump for flow generation of the liquid medium, a syringe pump with a 500 µL syringe (with a 1 mm inner diameter tube being fixed to its outlet) for injecting the suspension of nanoparticles into the tubing (inner diameter – 2 mm) leading to the glass tube (inner diameter – 1 mm) being positioned between the magnetic circuit. The magnetic circuit (Fig. 4) generating a DC magnetic field gradient along the length of the glass tube consisted of 10 permanent neodymium magnets (20 mm × 20 mm × 20 mm), disposed in two adjacent one to another frames being made of Plexiglas material (no magnetic items were used in the frame structure). A microscope was used to observe the behaviour of particles at several distinct points along the fluid flow path between said frames with permanent magnets disposed therein.

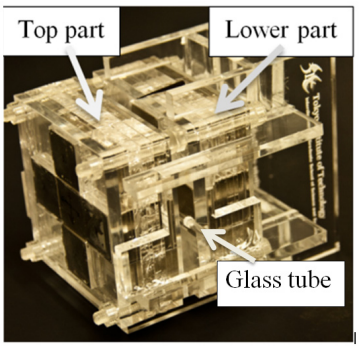

Fig. 4. Permanent magnets enclosed in a plastic frame: assembled magnetic device

3. RESULTS

The properties of targeting environment were chosen such that it would at least partially resemble any blood vessel in human's body. Assessment of flow of magnetic particles between two magnetic parts of the targeting device was done in a 1.5 % PVP (grade K90) solution. This gave viscosity of between 3×10^{-3} Pa·s and 4×10^{-3} Pa·s which is the viscosity of arterial blood. In a flowing liquid with viscosity of a blood an additional phenomena [11] helps to move particles toward the vessel walls assisting in trapping drug-carrying particles. In the experiment the flow rate was (1 – 10) mL/min, the diameter of lumen of said flow path was 2 mm; these are parameters that approximate the *arteria radialis* located in an arm.

Monitoring the flow of particles in between the two elements of the magnetic device was done at initial supply of main stream liquid at a rate of 1 mL/min. By using such low flow rate of main stream liquid (compared to target rate of 20 mL/min, which is characteristic for the radial arteries in arms) it was easy to observe close-to-desirable behavior of FePt particles; the bigger were the particles and/or clusters thereof the more effectively they were trapped in the device at an increased flow rates of the main stream (volume of the injected particles is directly proportional to the attraction force of the magnetic field source). Trajectory and sedimentation of FePt particles was

observed along three lines parallel to the inner surfaces of the device (Fig. 5).

First position. Distance of longitudinal center line of a glass tube from the surface of the top part of magnetic device was 3.5 mm and from the surface of the lower part was 11.5 mm. At the initial moment of injection of solution of FePt particles into the main stream particles started rapidly accumulating at three clearly defined positions. First aggregation area of about 10 mm in length and about 1 mm in height had formed to the left from the center of the 1st magnet (near the inlet) and the second aggregate (center of the 2nd magnet) was approximately of the same length but slightly of lower high. Certain amount of particles were carried from two primary aggregation areas by the stream thus forming the third aggregation near the edge of the 3rd magnet approximately in the length from its middle to its edge (near the outlet end of the glass tube). This was expected because the magnetic field gradient is elevated at these sections due to polarity direction of magnets of opposing sides at each of these areas. After injection of the magnetic suspension was stopped shape of the three aggregates didn't change significantly with time. This indicates that the magnetic device creates three strongly defined aggregation areas whereat most of the injected particles are rendered immobile.

Fig. 5. Position of glass tube relative to the inner surfaces of the magnetic device (left block – top part; right block – lower part) at 1st position, 2nd position, and 3rd position

First aggregate started to show a sign of wash-off after 10 min after injection of nanoparticles was stopped. This was allowed to progress for 22 minutes (Fig. 6, a). At the 23 min time mark after stopping the injection of FePt particles no considerable degradation in size of second aggregate (Fig. 6, b) was observed. Length of the aggregate was about 5 mm to both sides from center of 2nd magnet where its height was about 1 mm at its highest point. The size of the second (Fig. 6, b) and third (Fig. 6, c) aggregates was not changing due to constant supply of particles from first and second aggregates, respectively. Increasing the PVP flow rate to 10 mL/min resulted in rapid wash-off of aggregations at all three positions. The pulsating flow produced by a roller pump resulted in uneven motion pattern of particles along the length of the glass tube. Each ending of produced pulse allowed particles to migrate backwards in the distance range of about 10 mm from the second aggregation, normally being pushed by the stream to the direction of the outlet. This effect was not observed at any other section of the glass tube.

In the first position a 150 μL of FePt based liquid suspension was supplied at flow rate of 50 μL/min. Previous experiment led to conclusion that it is more efficient in terms of captured particles to supply certain quantity of particles at a higher input flow rate than the same quantity at a lower rate. This is due to the interaction of magnetic field and particles: lower concentration of particles per certain volume of flowing liquid gives weaker magnetic interaction between particles thus weaker overall effect of the magnetic field gradient to said particles. Greater concentration allows faster formation of an anchor body (bulk of suspended particles) whereat the magnetic force of the anchor attracts the inlet particles causing their velocity to increase. It has been determined both experimentally and theoretically that particles moving faster than local shear flow will experience additional forces toward the walls of a vessel [11].

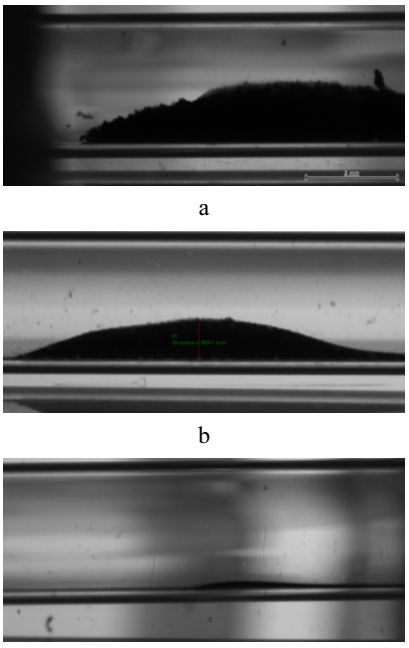

Fig. 6. Build-ups of FePt particles: a – first region after 22 min after the feed of FePt particles was stopped; b – 2nd aggregate after 23 min of stopped injection of FePt; c – 3rd aggregate after 24 min of stopped injection of FePt

Second position. The longitudinal center line of the glass tube was disposed at the distance of about 7 mm from inner surfaces of both parts of the magnetic device. The aggregates formed after injecting 50 μL – 100 μL of FePt particles. Turbulent areas were observed downstream from both first and second aggregates (Fig. 7) after supply of 150 μL of magnetic suspension has been stopped. Subsequent images were captured after 10 min after main stream flow has been stopped (Fig. 8).

Third position. At this instance, distance from the inner surface of the lower part and the top part of magnetic device to the longitudinal center line of the glass tube was 6.5 mm and 8.5 mm, respectively. Particles migrated (Fig. 9, a) from a side of the glass tube which was closer to the top part of the device, to the side that was closer to the

lower part. The area of transition from first aggregation to the second/middle aggregation (Fig. 9, b) had formed around the middle of the first magnet.

Evident migration of clusters of considerable size mainly at the upper layer of the aggregate was observed (Fig. 9, c, d) after a few minutes following the stopping of injection of particle. In Fig. 9, b, length of 2nd aggregate's main body was observed to be about 5 mm, but the major spread was about 10 mm long from the center of the 2nd magnet. A steady migration back to the bulk of particles, which had settled on a wall of the glass tube right after (in the distance up to 5 mm) the 2nd aggregate, was observed. Particles that had settled at the wall further than about 5 mm from the bulk of particles were washed away by the stream. After the main stream was stopped the 2nd aggregate (Fig. 9, e) in the third position of the glass tube particularly resembled the 2nd aggregate, observed in the second position (Fig. 8, b) of the glass tube.

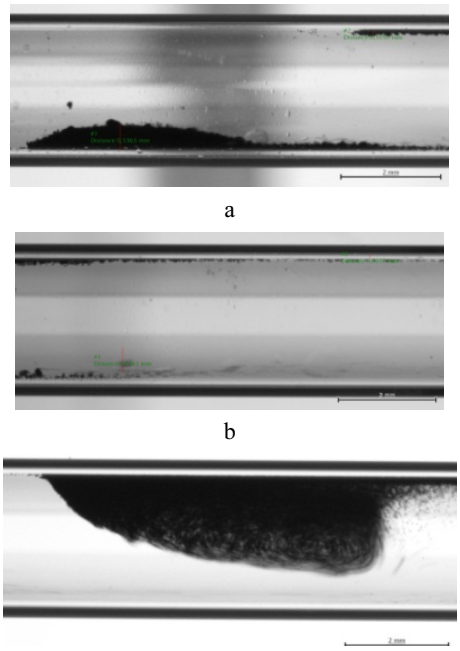

a

b

c

Fig. 7. Injection of particles is stopped for 20 min: a – 1st aggregate; b – following area just beyond first aggregate; c – 2nd aggregate

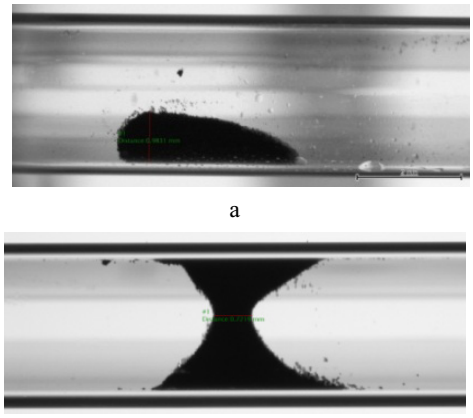

a

b

Fig. 8. Main-stream flow is stopped: a – 1st aggregate; b – 2nd aggregate

4. DISCUSSION AND CONCLUSIONS

Main research idea was to investigate whether the applied magnetic forces can compete with convective blood (drag) forces that tend to wash particles away, regarding active magnetic drug delivery technique. As magnetic force on a particle is strongly dependent on the size of the particle (i. e., the force is proportional to d^3, where d is the diameter of the particle), many studies have consequently focused on micron-sized magnetic particles [1, 4, 15]. But particles having diameter of 10 μm and more are not suitable for in vivo applications since they would obstruct the blood capillaries [1]. The blood flow drag forces on magnetic particle vary with its position in the blood vessel. A particle at the vessel centerline will experience a higher blood velocity and hence a higher drag force, but a particle near the blood vessel wall will be surrounded by a near zero blood velocity. Thus a particle near a vessel wall will experience a much smaller drag force and can potentially be held by a much smaller magnetic force.

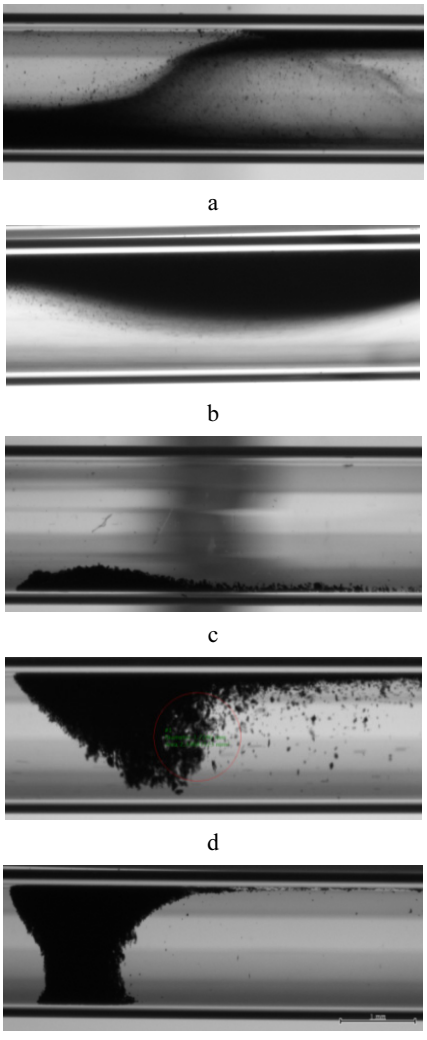

a

b

c

d

e

Fig. 9. Formations at the third position: a – transition from 1st aggregate to 2nd; b – 2nd aggregation area; c –1st aggregate and transition of particles to the 2nd aggregate; d – 2nd aggregate; e – 2nd aggregate after supply of FePt suspension has been stopped for 50 min (main stream has also been stopped)

Research showed that using the special order of permanent magnets it is possible to create magnetic field gradient sufficient enough to trap a significant portion of FePt particles being in the 50 nm – 100 nm size range at a specific location. Moreover, it was also shown that carriers can easily be aggregated in liquid having viscosity between 3×10^{-3} Pa·s and 4×10^{-3} Pa·s at the flow rate of up to 10 mL/min. The targeting distance was only about 0.5 cm, but it has been reported that this is normal achievable distance for targeting research so far [1]. Produced magnetic field of used magnetic device as well as reached gradient values was well in the range of applicable means for magnetic drug targeting research [1, 8, 9]. Moreover, use of special ordered magnets with relatively smaller dimensions (for composing a Halbach array type assembly) is more advantageous than using relatively large permanent magnets; although increase in size of magnets means increase in generated magnetic field values further from surface of a magnet, but the use of larger magnets to extend the magnetic field to deeper regions may not resolve the problem since low magnetic field gradients tend to result. The particle trajectory and aggregation at the point of interest allow concluding that device is well suited for magnetic drug targeting application because major amount of injected particles was retained within the area of targeting. Obtained information defines two major branches for further development, that is to redesign the device so that deeper than 0.5 cm targeting would be achieved, and use larger than 50 nm in diameter, in particular in the range of 100 nm – 200 nm in diameter, Fe_3O_4 particles. These two aspects will be considered as particularly contributing to effective deep magnetic drug targeting.

REFERENCES

1. **Lubbe, A. S., Alexiou, C., Bergemann, C.** Clinical Applications of Magnetic Drug Targeting *Journal of Surgical Research* 95 (2) 2001: pp. 200 – 206.
2. **Jurgons, R., Seliger, C., Hilpert, A., Trahms, L., Odenbach, S., Alexiou, C.** Drug Loaded Magnetic Nanoparticles for Cancer Therapy *Journal of Physics: Condensed Matter* 18 (38) 2006: pp. S2893 – S2902.
3. **Taylor, E. N., Webster, T. J.** Multifunctional Magnetic Nanoparticles for Ortho-pedic and Biofilm Infections *International Journal of Nanotechnology* 8 (1/2) 2011: pp. 21 – 35.
4. **Kempe, M., et al.** The Use of Magnetite Nanoparticles for Implant-assisted Magnetic Drug Targeting in Thrombolytic Therapy *Biomaterials* 31 (36) 2010: pp. 9499 – 9510.
5. **Jordan, A., Scholz, R., Maier-Hauff, K., van Landeghem, F. K., Waldoefner, N., Teichgraeber, U., Pinkernelle, J., Bruhn, H., Neumann, F., Thiesen, B., von Deimling, A., Felix, R.** The Effect of Thermotherapy Using Magnetic Nanoparticles on Rat Malignant Glioma *The* Journal *of* Neuro-Oncology 29 2005: pp.1 – 8.
6. **Schuell, B., et al.** Side Effects During Chemotherapy Predict Tumour Response in Advanced Colorectal Cancer *British Journal of Cancer* 93 (7) 2005: pp. 744 – 748.
7. **Chertok, B., et al.** Iron Oxide Nanoparticles as a Drug Delivery Vehicle for MRI Monitored Magnetic Targeting of Brain Tumors *Biomaterials* 29 (4) 2008: pp. 487 – 496.
8. **Takeda, S., Mishima, F., Fujimoto, S., Izumi, Y., Nishijima, S.** Development of Magnetically Targeted Drug Delivery System Using Superconducting Magnet *Journal of Magnetism and Magnetic Materials* 311 (1) 2007: pp. 367 – 371.
9. **Nacev, A., Beni, C., Bruno, O., Shapiro, B.** The Behaviors of Ferromagnetic Nano-particles in and Around Blood Vessels Under Applied Magnetic Fields *Journal of Magnetism and Magnetic Materials* 323 (6) 2011: pp. 651 – 668.
10. **Ally, J., Martin, B., Behrad Khamesee, M., Roa, W., Amirfazli, A.** Magnetic Targeting of Aerosol Particles for Cancer Therapy *Journal of Magnetism and Magnetic Materials* 293 (1) 2005: pp. 442 – 449. http://dx.doi.org/10.1016/j.jmmm.2005.02.038
11. **Forbes, Z. G., Yellen, B. B., Barbee, K. A., Friedman, G.** An Approach to Targeted Drug Delivery Based on Uniform Magnetic Fields *IEEE Transactions on Magnetics* 39 (5) 2003: pp. 3372 – 3377.
12. **Hayden, M. E., Hafeli, U. O.** Magnetic Bandages for Targeted Delivery of Therapeutic Agents *Journal of Physics: Condensed Matter* 18 (38) 2006: pp. S2877 – S2891. http://dx.doi.org/10.1088/0953-8984/18/38/S23
13. **Zheng, J., Wang, J., Tang, T., Li, G., Cheng, H., Zou, S.** Experimental Study on Magnetic Drug Targeting in Treating Cholangiocarcinoma Based on Internal Magnetic Fields *The Chinese–German Journal of Clinical Oncology* 5 (5) 2006: pp. 336 – 338.
14. **Holligan, D. L., Gillies, G. T., Dailey, J. P.** Magnetic Guidance of Ferrofluidic Nanoparticles in an in Vitro Model of Intraocular Retinal Repair *Nanotechnology* 14 (6) 2003: pp. 661 – 666.
15. **Goodwin, S., Peterson, C., Hoh, C., Bittner, C.** Targeting and Retention of Magnetic Targeted Carriers (MTCs) Enhancing Intra-arterial Chemotherapy *Journal of Magnetism and Magnetic Materials* 194 1999: pp. 132 – 139. http://dx.doi.org/10.1016/S0304-8853(98)00584-8
16. **Jayagopal, A., Linton MacRae, F., Fazio, S., Haselton, F. R.** Insights Into Atherosclerosis Using Nanotechnology. Springer Science, BusinessMedia, LLC2010 Curr Atheroscler Rep., 2010: pp. 12:209 – 215.
17. **Forbes, Z. G., Yellen, B. B., Halverson, D. S., Fridman, G., Barbee, K. A., Friedman, G.** Validation of High Gradient Magnetic Field Based Drug Delivery to Magnetizable Implants Under Flow *IEEE Transactions* on *Biomedical Engineering* 55 (2) Pt 1 Feb. 2008: pp. 643 – 649.
18. **Robertson, W., Cazzolato, B., Zander, A.** Parameters for Optimizing the Forces Between Linear Multipole Magnet Arrays *IEEE Magnetics Letters* Volume 1 2010.
19. **Hafeli, U. O., Gilmour, K., Zhou, A., Lee, S., Hayden, M. E.** Modeling of Magnetic Bandages for Drug Targeting: Button vs. Halbach Arrays *Journal of Magnetism and Magnetic Materials* 311 (1) 2007: pp. 323 – 329. http://dx.doi.org/10.1016/j.jmmm.2006.10.1152
20. **Raich, H., Blumler, P.** Design and Construction of a Dipolar Halbach Array with a Homogeneous Field from Identical Bar Magnets: NMR Mandhalas. Concepts in *Magnetic Resonance Part B* (*Magnetic Resonance Engineering*) Vol. 23 B (1) 2004: pp. 16 – 25.
21. **Katter, M.** Angular Dependence of the Demagnetization Stability of Sintered Nd-Fe-B Magnets *Proceedings of the Magnetics Conference, 2005. INTERMAGAsia 2005. Digests of the IEEE International* 2005: pp. 945 – 946.
22. **Tsai, K. L., Pickard, D., Kao, J., Yin, X., Leen, B., Knutson, K., Kant, R., Howe, R. T.** Magnetic Nanoparticle-driven Pumping in Microchannels. Transducers 2009, Denver, CO, USA, June 21 – 25, 2009.